2011

Application Of Kalman Filter With Time Correlated Measurement Errors In Subsurface Contaminant Transport Modeling

Godfrey Mills
North Carolina Agricultural and Technical State University

APPLICATION OF KALMAN FILTER WITH TIME CORRELATED MEASUREMENT ERRORS IN SUBSURFACE CONTAMINANT TRANSPORT MODELING

by

Godfrey Mills

A thesis submitted to the graduate faculty
in partial fulfillment of the requirements for the degree of
MASTER OF SCIENCE

Department: Civil and Environmental Engineering
Major: Environmental Engineering
Major Professor: Dr. Shoou-Yuh Chang

North Carolina A&T State University
Greensboro, North Carolina
2011

School of Graduate Studies
North Carolina Agricultural and Technical State University

This is to certify that the Master's Thesis of

Godfrey Mills

has met the thesis requirements of
North Carolina Agricultural and Technical State University

Greensboro, North Carolina
2011

Approved by:

Dr. Shoou-Yuh Chang Major Professor	Dr. Stephanie Luster-Teasley Committee Member
Dr. Manoj K. Jha Committee Member	Dr. Sameer A. Hamoush Department Chairperson

Dr. Sanjiv Sarin
Dean of Graduate Studies

BIOGRAPHICAL SKETCH

Godfrey Mills was born on November 17, 1979, in Takoradi, Ghana, West Africa. He received his Bachelor of Science degree in Agriculture Engineering from Kwame Nkrumah University of Science and Technology, Ghana in 2004 and a Master of Science degree in Water Resources Engineering and Management from Kwame Nkrumah University of Science and Technology, Ghana in 2008. He is a candidate for the Master of Science degree in Civil Engineering.

ACKNOWLEDGEMENTS

First and foremost I would like to thank my advisor Dr. Shoou-Yuh Chang. I appreciate all his contributions of time, ideas, and funding towards this research. I would also like to show my appreciation to Dr. Stephanie Luster-Teasley and Dr. Manoj K. Jha for serving on my thesis committee panel. I gratefully acknowledge the support and assistance of my fellow graduate students and faculty members in the Civil and Environmental Engineering Department. Finally I would like to acknowledge my family especially my uncle, Isaac Kelly Ackun and my mother Elizabeth Kuma Mills for their moral support, love and encouragement. This work was sponsored by the Department of Energy Samuel Massie Chair of Excellence Program under Grant No. DF-FG0194EW11425.

TABLE OF CONTENTS

LIST OF FIGURES

FIGURES **PAGE**

LIST OF SYMBOLS

a	correlation coefficient for measurement error
$\mathbf{b}$	aquifer thickness
$\mathbf{\Phi}$	state transition matrix
$\mathbf{S}$	correlation coefficient matrix
EKF	Extended Kalman filter
KF	Kalman filter
RMSE	root mean square error
PNSD	process noise standard deviation
SDON	standard deviation of observation noise
FTCS	forward time central space
FD	finite difference
$\mathbf{H}$	sensitivity matrix
$\mathbf{Q}$	process noise covariance
$\mathbf{R}$	measurement noise covariance
$\mathbf{x}_t$	state vector describing the concentration plume at epoch t
$\mathbf{w}_t$	the model process noise at epoch t
$\mathbf{\Omega}$	square boundary
$\mathbf{v}_t$	observation noise at epoch t
$\mathbf{v}$	average linear groundwater velocity

$\mathbf{z}_t$	state vector for observed data at epoch *t*
$\mathbf{K}_{t+1}$	Kalman gain matrix
$\mathbf{P}_t$	optimal estimate error covariance matrix at epoch *t*
$\mathbf{L}_t$	observations with time-correlated errors at epoch *t*
$\mathbf{A}_t$	design matrix for the time correlated measurement
$\mathbf{u}$	time correlated noise
$\mathbf{n}$	white measurement noise
$\mathbf{S}$	correlation coefficient
$\boldsymbol{\varepsilon}$	white noise component for the correlated measurement errors
$\mathbf{C}_t$	correlation between $\mathbf{v}_t$ and $\mathbf{w}_t$
$\mathbf{R}_t$	covariance matrix of the measurement noise
$\mathbf{M}$	covariance matrix of $\boldsymbol{\varepsilon}$
$\mathbf{N}$	covariance matrix of $\mathbf{n}$
GPS	geographic positioning system
$\mathbf{D}_x$	hydrodynamic dispersion coefficient in *x* direction
$\mathbf{D}_y$	hydrodynamic dispersion coefficient in *y* direction
$\boldsymbol{\mu}$	porosity
$\mathbf{C}$	conservative solute concentration
$\mathbf{M}_o$	initial mass of contaminant per unit area
C_0	initial concentration of pollutant

$\mathbf{N_t}$	total number of sampling nodes
$\mathbf{C(x,y,t)}$	reference true value of concentration
$\mathbf{C^E(x,y,t)}$	estimated value of concentration
$\mathbf{t}$	time

ABSTRACT

Mills, Godfrey. APPLICATION OF KALMAN FILTER WITH TIME CORRELATED MEASUREMENT ERRORS IN SUBSURFACE CONTAMINANT TRANSPORT MODELING.**(Major Professor: Dr. Shoou-Yuh Chang)**, North Carolina Agricultural and Technical State University.

Contaminant transport modeling of a conservative solute in the subsurface is investigated by applying a Kalman filter (KF) with time correlated measurement errors. The usual method or assumption often employed is white Gaussian errors, but time correlated measurement errors were used instead for this research, since some hydrological observation data exhibit time correlated error characteristics.

An observation data was generated from a two dimensional analytical solution with an additive time correlated random errors. This was used as the measurement Equation for the KF with time correlated measurement errors and the KF with white Gaussian errors. The measurement differencing algorithm was adopted in deriving a discrete time varying KF with time correlated measurement errors for a two-dimensional contaminant transport prediction in the subsurface. An expression for the correlation coefficient matrix for colored noise, termed as "Time correlated operator matrix", is derived instead of using a traditional diagonally assigned one. A computer code was generated for both KF with white Gaussian errors and KF with time correlated errors.

Simulation results indicated an improved root mean square error (RMSE) profile of KF with time correlated errors over KF with white Gaussian errors. The KF with correlated errors reduced the errors in prediction by 11.4% compared to the KF with

white Gaussian errors using only 9 observation points in the entire 20×20 space domain. Further investigation revealed that the performance of the KF with time correlated observation errors was improved when the measurement errors standard deviation was reduced.

CHAPTER 1

INTRODUCTION

Contaminant transport in the subsurface is an area of keen interest. The groundwater resource is a valuable asset that needs protection because of its usefulness to humans, the important role it plays in hydrological processes such as base-flow and also its vulnerability to pollutants. Some communities and cities in the United State of America depend solely on groundwater for water supply. It was estimated in 2005, that out of the total water withdrawn in the US, 20% constituted groundwater (USGS 2009). However, there are instances that this resource suffers from severe pollution due to natural causes or by human activity. In most cases, little or no attention is paid to the impact of industrial activities on the groundwater resource, leading to this vital resource becoming polluted. In view of this, an in depth understanding of the dynamics within the subsurface is an important tool that can effectively be employed in the wake of a pollution event.

The complex nature of groundwater systems makes it difficult to successfully predict the fate and transport of contaminant. Due to this, measurement of aquifer parameters and contaminant plume concentrations from the field may be localized, not representing the entire system or even erroneous. Apart from this, it is difficult, time consuming and expensive to have an accurate estimate of the extent of pollution in a groundwater resource just by field measurements. For a cost effective remediation activity of such contaminated aquifers, it is essential to obtain a somewhat accurate

knowledge of the extent of the pollution in time and in space in a manner that eliminates or reduces the prediction error. This has led to a lot of research on the fate and transport of contaminant in subsurface (Hossain and Yonge 1997; Ganguly et al. 1998; Solo-Gabriele 1998; Rabideau and Khandelwal 1998; Lee 2004; Yan et al. 2006; Zou and Parr 1995). Mathematical models for contaminant transport in the subsurface are widely used. Such models offer information on areas in the subsurface that would have otherwise been impossible to obtain information with field equipment. The results obtained are somewhat relevant but not accurate enough to characterize the subsurface. A better way of obtaining accurate results is by data assimilation. This approach aims at adding extra information from field measurement to the mathematical model for improved prediction.

Data assimilation is a technique that can be employed for parameter estimation and improving model accuracy. It involves a combination of the observational data and the underlying dynamical principles (Equations) governing the system under observation for an accurate prediction (Robinson and Lermusiaux 2000). On the contrary, the strength of the data assimilation for parameter estimation can be its weakness as well, since the results are forced towards the observation, it is possible to introduce algorithms that are theoretically correct but the resulting model may be unstable. It is of importance to confirm the assumptions made in the model in order to prevent a forcing that results in an unstable model (Drecourt 2003). Parameter estimation techniques come in many forms, depending on the specific goals and aims of the user. The three most relevant goals are model improvement, the study of dynamical processes through state estimation, and forecast improvement. Model improvement implies refining parameters or inputs to the

model. The general idea is to ask what set of parameters would best reproduce the observations, thus the name parameter estimation. Inverse theory is another traditional name, especially when referring to solid-earth geophysics where the systems are considered time independent (Paola and Eli; 1996).

The main objectives for this research are to:

1. Investigate the predictive performance of KF with colored measurement errors in subsurface contaminant transport modeling using a conservative solute.

2. Compare the performance of the conventional discrete KF with white Gaussian noise versus the KF with colored measurement noise in contaminant transport prediction in the subsurface.

CHAPTER 2

LITERATURE REVIEW

The Kalman filter (KF) is a data assimilation technique that is able to process data recursively to generate optimum estimates of the state. The KF can be used for past, present and future state estimates (Welch and Bishop 2006). The KF has been used in subsurface pollutant transport and groundwater flow modeling for last three decades (Chang and Jin 2005; Eppstein and Dougherty 1996; Ferraresi et al. 1996; Geer 1982; Graham and McLaughlin 1989; Pimentel et al. 1982; Van Geer and Van Der Kloet 1985; Van Geer et al. 1991; Zou and Parr 1995). Its effectiveness and efficiency is due to its ability to handle dynamic and stochastic processes, providing optimal solutions for linear systems (Chang and Jin 2005). In applying the KF for contaminant transport estimation, it was assumed the process and measurement noise were white Gaussian, implying zero mean, uncorrelated and flat or constant power spectral density. Additionally, Chang and Latif (2007) applied Kalman and Particle filters to effectively predict a one dimensional leachate transport model and also used an Extended Kalman filter (EKF) to improve the accuracy of a two dimensional subsurface contaminant transport model for a conservative solute (Chang and Latif 2010). In some other areas of hydrology, the KF was applied with the assumption of white Gaussian noise (Yu et al. 1989; Ngan and Russel 1986). Most applications of KF in hydrology not mentioned here have been done based on white Gaussian noise assumptions. Contrary to traditional knowledge, this assumption is not always valid. In certain situations it makes more sense to consider

colored noise or correlated errors instead of white noise, especially for cases where measurement data were found to contain correlated errors.

It is a priority to simulate stochastic process to closely represent the system under study. As such, application of correlated errors is vital in the accurate simulation of varied physical systems which exhibit such characteristics. Some of the areas correlated errors have been applied include physical, chemical and biological systems (Van Kampen 1992; Huang et al. 2010; Billah et al. 1990). In an earlier application, Johnson (1970) applied the KF with colored-noise to a nonlinear system and a nonlinear observation model, with the assumption of a linear estimator. The Equations used in this earlier application were based on previously developed formulae; including the colored measurement noise statistics and the statistics of non-estimated model parameter errors. He compared several simulations made with this filter and results of an estimation procedure constructed with the utilization of the standard white noise assumptions. The difference between the KF with white-noise results and the KF with colored-noise results were found to be minimal. Another study on the influence of surface and soil moisture processes on atmospheric precipitation and radioactive forcing on soil moisture was conducted by Wang et al. (1997) based on non-Gaussian colored-noise. It was observed that soil moisture for climatic regions with larger land-atmospheric positive feedback have large correlation time scales. The KF with correlated errors has, with equal success been applied to predict flooding events in the occurrence of rainfall. Colored-noise was added to a KF to effectively control the divergence of the filter for predicting rainfall and river flow models in the event of flooding. An autoregressive moving average model was

fitted to hourly rainfall to enable the prediction. These two systems were connected in a series to form a state-space system which was then used in the KF algorithm with colored-noise to correct and update the estimated state variables (Wang et al. 1999). Another area correlated errors have been used is in the study of the movement of continental-scale water balance in the central United States. Two separate models of white noise and colored noise were designed based on available atmospheric data. The results indicated that time correlated atmospheric moisture fluctuation removes the bimodality of the soil moisture probability distribution and that, the correlated-error approach successfully captured the water balance dynamics in the study region despite the absence of multiple soil moisture states (Kochendorfer and Ramirez 2003).

In the ensuing years, application of time correlated measurement and process noise in hydrological modeling was suggested by Drecourt (2003) especially in the use of GPS equipments for field measurements. In support of this claim, Kuhlmann (2003) obtained some GPS observations results with high sampling rate that were time correlated. In the case of Kuhlmann (2003), a KF with shaping filter was applied in a GPS time series to simulate these correlated measurement errors which yielded good results. Later, a novel approach to the setup of a KF using an automatic calibration framework for estimation of covariance matrices was presented by Drecourt et al. (2006). This method was applied to a twin-test experiment with a groundwater model and a colored noise KF. The results indicated that lattice sampling was more favorable than the usual Monte Carlo simulation because its ability to preserve the theoretical mean reduces the size of the ensemble needed. The resulting KF with colored noise proved to be

efficient in correcting dynamic errors and bias over the whole domain studied. The uncertainty analysis provided a reliable estimate of the error in the neighborhood of assimilation points but the simplicity of the covariance models led to underestimation of the errors far from assimilation points. In a different area of application, Kumar et al. (2007) also used a colored-noise KF to diminish the error effects caused by GPS sensors placed on vibrating structures. Effects due to vibration were added and a colored-noise filter was designed to mitigate the effects of the beacon movements on state estimation. The sensitivity analysis conducted indicated that the colored-noise filter provides significant improvements over a filter that does not account for vibrational effects. Additionally, Charles et al. (2008) used colored noise as the driving force to simulate contaminant transport in shallow waters. The Colored noise was used because initial application of white noise could not accurately account for the short-term dispersion of contaminants. In this investigation, the particle model with an additive colored noise was used to simulate the contaminant transport process to improve the results of the model shortly after the contaminant is deployed.

In the application of KF with colored or correlated noise, the process noise may be colored, the measurement noise may be colored or both of them may just be correlated (Simon 2006). The derivation of the algorithm for colored noise in KF originally involved the state augmentation method as explained by Brown et al. (1997), Welch et al. (2006) and Gelb (1974). But, this method increases the complexity of the algorithm, making the state variable two dimensional and also increasing the computational difficulty for systems with large matrix dimensions. Another problem is the difficulty of

implementing this method in the case of correlated measurement errors because of the instability of the Kalman gain matrix $\mathbf{K_t}$ (Bryson and Henrikson 1968; Gelb 1974; Popescu and Zeljkovic 1998; Sun and Deng 2004). In overcoming these short comings, Wang et al. (2010) proposed the Perturbed-P algorithm to make it possible to apply the state augmented method while avoiding the problem of a singular error covariance matrix $\mathbf{P_t}$. Petovello et al. (2009) also presented a new algorithm for considering time-correlated measurement errors in KF. This algorithm was derived based on the measurement-differencing concept, originally formulated by Bryson and Henrikson (1968). The difference between the original algorithm and the modified one by Petovello et al. (2009) lies in the numerical competence of the latter one. Also, the new algorithm gives full consideration to additive white noise which is often still present but ignored in the previous implementation of KF with colored-noise algorithm. Simulated results based on this new algorithm yielded more realistic results than the previous algorithm based on the measurement differencing method.

CHAPTER 3

METHODOLOGY

The methodology employed in this research involves a consideration of the numerical (an explicit finite difference method), analytical (which is used as a reference true solution), KF with white Gaussian noise and finally KF with colored measurement noise results. Comparison is made between the four results relative to the true solution to find their effectiveness and usefulness in state estimation in subsurface contaminant transport.

3.1 Numerical Solution Approach

The classical advection-dispersion equation is solved numerically using Forward Time and Central-Space (FTCS) method as used by Chang and Jin (2005). Making use of the two dimensional version of the governing solute transport equation (Equation-1), the concentration of the conservative solute will be determined for each time step and their corresponding plume spread in the subsurface porous media.

$$\frac{\partial \mathbf{C}}{\partial \mathbf{t}} = \frac{\mathbf{D}_y \partial^2 \mathbf{C}}{\mathbf{R} \partial \mathbf{y}^2} + \frac{\mathbf{D}_x \partial^2 \mathbf{C}}{\mathbf{R} \partial \mathbf{x}^2} - \mathbf{v} \frac{\partial \mathbf{C}}{\mathbf{R} \partial \mathbf{x}} \tag{1}$$

t = Time (T),

R = Retardation

D = Coefficient of hydrodynamic dispersion (L^2T^{-1}),

v= Average linear pore water velocity in the x direction (LT^{-1}),

C= Conservative solute concentration (ML^{-3}).

At a non-steady state, the solution of the equation is found by finding the partial differential solution for each of the partial differential terms using a numerical solution approach. The approximate solution for each term in the advection-dispersion equation is then computed using FTCS method. This gives an approximate solution since it involves truncation and other numerical errors.

3.2 Reference True Solution Approach

The two dimensional analytical solution for pulse input is adopted as the reference true solution for this research work (Schwartz and Zhang; 1994). This model assumes a homogeneous, isotropic aquifer with a non-steady state in a two dimensional flow field. The advection-dispersion equation will be used to determine the changes in concentration with respect to time and space in the subsurface. It is assumed that spill occurs instantaneously as a plane source.

$$C(x, y, t) = \frac{M_o}{4\pi b \mu t \sqrt{D_x D_y}} e^{-\left[\frac{(x - vt/R)^2}{4D_x t/R} + \frac{y^2}{4D_y t/R}\right]} \quad (2)$$

Where,

$\mathbf{C}$ = Conservative solute concentration (ML^{-3}),

$\mathbf{x}$ = Distance (L) in x direction

$\mathbf{y}$ = Distance (L) in y direction

$\mathbf{t}$ = Time (T),

$\mathbf{D_x}$ = Constant horizontal hydrodynamic dispersion coefficient ($L^2\ T^{-1}$),

$\mathbf{D_y}$ = Constant vertical hydrodynamic dispersion coefficient ($L^2\ T^{-1}$),

$\mathbf{R}$ = Retardation constant

$\boldsymbol{\mu}$ = Porosity

$\mathbf{b}$=Aquifer thickness (L)

$\mathbf{v}$= Average linear pore water velocity (LT^{-1})

Equation-2 represents the changes in time and distance in concentration, depending on the initial mass of contaminant per unit area ($\mathbf{M_o}$) injected uniformly across the aquifer cross section during a spill at time $\mathbf{t}$ =**0**. It is assumed that the aquifer has a uniform cross section area. The boundary condition of the two dimensional mass transport with an instantaneous point source is expressed as,

$$\mathbf{M(x, y, t)}\big|_{t=0} = \mathbf{M_0(x = x_i, y = y_i)}$$

$$\mathbf{C(x, y, t)}\big|_{t=0} = \mathbf{C_0(x = x_i, y = y_i)}$$

$$\mathbf{C(x,\ y,\ t)}\big|_{\Omega} = \mathbf{0}$$

Where, (x_i, y_i) is the initial co-ordinate that the pulse input occurred and Ω is a square boundary.

3.3 Kalman Filter

The Kalman filter (KF) as introduced in 1960 by Rudolf Emile Kalman in his publication for use in electrical control systems is a widely used method for deformation analysis nowadays. It serves as a recursive solution to the discrete-data linear filtering problem. This estimation procedure can still be done even when the precise nature of the modeled system is not known (Welch and Bishop 2006). The recursive model is based on a Markov chain with operators disturbed by Gaussian error. For every time step the new state is generated based on a combination of the old state and added Gaussian error (Welch and Bishop 2006).

Random noise or error is most of the time applied to subsurface systems to reflect their heterogeneous nature so that a model can have characteristics close to the subsurface in order to have more accurate results. The state-space model is governed by process equation and measurement equation, which are required in order to run the KF.

3.3.1 Process Equation

In the application of KF in contaminant transport modeling in the subsurface, the process equation is a slight modification of the linear numerical model of the advection dispersion differential equation employed in the subsurface contaminant transport equation. The modification involves the addition of an error term as shown in Equation-3.

$$\mathbf{x}_{t+1} = \mathbf{\Phi x}_t + \mathbf{w}_t \quad (3)$$

Where, $\mathbf{x}_{t+1}$ is the state vector describing the concentration plume at epoch $\mathbf{t+1}$; $\mathbf{\Phi}$ is the State Transition Matrix; $\mathbf{x}_t$ is the state vector describing the previous concentration plume at epoch $\mathbf{t}$; $\mathbf{w}_t$ is the model process noise or system error with covariance matrix $\mathbf{Q}_t$ and zero mean.

3.3.2 Measurement Equation

In the absence of field data, the analytical solution was adopted as the true solution for this study. This assumption is justified since the true solution in reality could be of any form. As in the case of Geogebeur and Pauwels (2007), synthesized data was employed as the true solution for their hydrologic parameter estimation using EKF. To make the analytical solution representative of a temporally correlated observation data, a time correlated (additive with time line) random error was added to the analytical solution for the whole experimental domain. This was used as the measurement equation for the KF with time correlated errors and the KF with white Gaussian errors. The observation equation for the entire domain is represented by Equation-4.

$$\mathbf{z}_t = \mathbf{H}\mathbf{x}_t^{\mathrm{T}} + \mathbf{v}_t \quad (4)$$

Where, $\mathbf{z}_t$ represents the state vector for all the observed data at all time steps; $\mathbf{H}$ denotes the measurement operator or design matrix; $\mathbf{v}_t$ is the error inherent in the observation

data with covariance $\mathbf{R}_t$ and zero mean; $\mathbf{x}_t^T$ is the transpose of the true value of the state vectors for all of the time steps.

3.4 Discrete Kalman Filter Algorithm

The KF works by estimating a process state using a form of feedback control. The Filter estimates the process state at some time and then obtains feedback in the form of noisy measurements. As such, the equations for the Kalman filter fall into two groups; time update or predictor equations and measurement update equations or corrector equations. The time update equations are responsible for projecting forward in time the current state and error covariance estimates to obtain the a priori estimates for the next time step. The measurement update equations are responsible for the feedback, in other words for incorporating a new measurement into the a priori estimate to obtain an improved a posteriori estimate (Welch and Bishop 2006). The KF Algorithm includes an optimal estimation equation for the stochastic process. This optimal estimate is given by the expression below;

$$\mathbf{x}_{t+1}^{(+)} = \mathbf{x}_{t+1}^{(-)} + \mathbf{K}_{t+1}\{\mathbf{z}_{t+1} - \mathbf{H}\mathbf{x}_{t+1}^{(-)}\} \tag{5}$$

The $\mathbf{K}_{t+1}$ denotes the Kalman gain matrix responsible for minimizing the optimal estimate error covariance matrix $\mathbf{P}_t$. The Kalman gain matrix is obtained from Equation-6.

$$\mathbf{K}_{t+1} = \mathbf{P}_{t+1}^{(-)}\mathbf{H}^{T}[\mathbf{H}\mathbf{P}_{t+1}^{(-)}\mathbf{H}^{T} + \mathbf{R}]^{-1} \quad (6)$$

The noise is advanced recursively for all time steps by Equation-7

$$\mathbf{P}_{t+1}^{(+)} = \mathbf{P}_{t+1}^{(-)} - \mathbf{P}_{t+1}^{(-)}\mathbf{H}^{T}[\mathbf{H}\mathbf{P}_{t+1}^{(-)}\mathbf{H}^{T} + \mathbf{R}]^{-1}\mathbf{H}\mathbf{P}_{t+1}^{(-)} \quad (7)$$

In this regard,

$$\mathbf{P}_{t+1}^{(-)} = \mathbf{\Phi}\mathbf{P}_{t+1}^{(+)}\mathbf{\Phi}^{T} + \mathbf{Q}_{t} \quad (8)$$

3.5 Kalman Filter with Time Correlated Measurement Errors

As stated earlier on, a prerequisite for optimal estimation using the KF is that the system has no time-correlated process and measurement errors in other words they are both white noise. However, this is not always the case in practice. There are certain cases that the errors have been found to be time correlated random errors. The algorithm or method in applying time correlated errors in Kalman filtering (KF) for contaminant transport in the subsurface is adopted from Petovello et al. (2009). Some advantages of this algorithm over other algorithms include:

1. This algorithm does not suffer from numerical problems or it does not yield systems whose transition matrices are near identity or ill-conditioned and does not increase the size or dimension of the state vector as proposed in the state augmentation approach by Gelb (1974).

2. This algorithm gives full consideration to additive white noise which in most case is ignored in other time correlated error algorithms.
3. It does not require reinterpretation of Kalman filter parameters. It is based on measurement differencing but does not have time latency problem.

In the case of observations $\mathbf{L}_t$ with time-correlated errors the observation is expressed in terms of the state vector and noise parameters as indicated in Equation-9.

$$\mathbf{L}_t = \mathbf{A}_t \mathbf{x}_t + \mathbf{u}_t + \mathbf{n}_t \tag{9}$$

Where, $\mathbf{A}_t$ represents the design matrix for the time correlated measurement, which is also equivalent to the design matrix $\mathbf{H}$ in Equation-4. The errors for the measurement equation consist of both colored and white additive noise $\mathbf{u}_t$ and $\mathbf{n}_t$, respectively. In the case of correlated errors, the colored noise vector of the observation has two components, colored part and white part as expressed in Equation-10.

$$\mathbf{u}_t = \mathbf{S}\mathbf{u}_{t-1} + \boldsymbol{\varepsilon}_{t-1} \tag{10}$$

Where, $\mathbf{u}_t$ is the colored noise vector at time step $\mathbf{t}$; $\mathbf{u}_{t-1}$ is the colored noise vector for previous time step; $\mathbf{S}$ is the state transition matrix containing the correlation coefficient. In the measurement differencing derivation explained by Simon (2006) he defines the $\mathbf{S}$ as a diagonal matrix with constant values ranging between 0 and 1. Setting the diagonal elements in $\mathbf{S}$ = 0 implies white noise, and any value other than 0 but less than 1 is a

characteristic of a particular time correlated measurement errors; $\boldsymbol{\varepsilon}_{t-1}$ is equivalent to the process noise vector for the correlated measurement error process, assumed to be uncorrelated with both $\mathbf{n}_t$ and the process noise vector $\mathbf{w}_t$. A new measurement equation based on the time difference approach is given by Equation-11.

$$\begin{aligned}\mathbf{z}_t &= \mathbf{L}_t - \mathbf{S}_t\mathbf{L}_{t-1} \\ &= \mathbf{A}_t\mathbf{x}_t + \mathbf{u}_t + \mathbf{n}_t - \mathbf{S}_t\left(\mathbf{A}_{t-1}\mathbf{x}_{t-1} + \mathbf{u}_{t-1} + \mathbf{n}_{t-1}\right) \\ &= \mathbf{A}_t\mathbf{x}_t + \left(\mathbf{S}_t\mathbf{u}_{t-1} + \boldsymbol{\varepsilon}_{t-1}\right) + \mathbf{n}_t - \mathbf{S}_t\left(\mathbf{A}_{t-1}\mathbf{x}_{t-1} + \mathbf{u}_{t-1} + \mathbf{n}_{t-1}\right) \\ &= \mathbf{A}_t\mathbf{x}_t + \boldsymbol{\varepsilon}_{t-1} + \mathbf{n}_t - \mathbf{S}_t\mathbf{A}_{t-1}\mathbf{x}_{t-1} - \mathbf{S}_t\mathbf{n}_{t-1}\end{aligned} \tag{11}$$

Equation 3 could be re-arranged in the form as shown in Equation-12.

$$\mathbf{x}_{t-1} = \boldsymbol{\Phi}_{t-1,t}^{-1}\left(\mathbf{x}_t - \mathbf{w}_{t-1}\right) \tag{12}$$

This is then substituted back into Equation-11 yielding a new Equation-13

$$\begin{aligned}\mathbf{z}_t &= \mathbf{A}_t\mathbf{x}_t + \boldsymbol{\varepsilon}_{t-1} + \mathbf{n}_t - \mathbf{S}_t\mathbf{A}_{t-1}\mathbf{x}_{t-1} - \mathbf{S}_t\mathbf{n}_{t-1} \\ &= \left(\mathbf{A}_t - \mathbf{S}_t\mathbf{A}_{t-1}\boldsymbol{\Phi}_{t-1,t}^{-1}\right)\mathbf{x}_t + \mathbf{S}_t\mathbf{A}_{t-1}\boldsymbol{\Phi}_{t-1,t}^{-1}\mathbf{w}_{t-1} - \mathbf{S}_t\mathbf{n}_{t-1} + \boldsymbol{\varepsilon}_{t-1} + \mathbf{n}_t\end{aligned} \tag{13}$$

Comparing Equation-13 and Equation- 4 it can be deduced that;

$$\mathbf{H} = \mathbf{A}_t - \mathbf{S}_t \mathbf{A}_{t-1} \boldsymbol{\Phi}^{-1}_{t-1,t} \tag{14}$$

$$\mathbf{v}_t = \mathbf{S}_t \mathbf{A}_{t-1} \boldsymbol{\Phi}^{-1}_{t-1,t} \mathbf{w}_{t-1} - \mathbf{S}_t \mathbf{n}_{t-1} + \boldsymbol{\varepsilon}_{t-1} + \mathbf{n}_t \tag{15}$$

The new covariance matrix of the measurement noise $\mathbf{R}_t$ is expressed as

$$\mathbf{R}_t = \mathbf{M}_{t-1} + \mathbf{N}_t + \mathbf{S}_t \mathbf{A}_{t-1} \boldsymbol{\Phi}^{-1}_{t-1} \mathbf{Q}_{t-1} \boldsymbol{\Phi}^{-T}_{t-1} \mathbf{A}^T_{t-1} \mathbf{S}^T_t \tag{16}$$

Where, $\mathbf{M}$ and $\mathbf{N}$ are the covariance matrices of $\boldsymbol{\varepsilon}$ and $\mathbf{n}$ respectively, or equivalently, the sum of the two covariance matrixes **M** and **N** is the same as **R** in Equation-6. Since the measurement error vector $\mathbf{v}_t$ is an explicit function of $\mathbf{w}_{t-1}$, it implies that these two error vectors $\mathbf{v}_t$ and $\mathbf{w}_t$ are correlated. The correlation is given by Equation-17.

$$\mathbf{C}_t = \mathbf{Q}_{t-1} \mathbf{S}^T \mathbf{A}^T_{t-1} \boldsymbol{\Phi}^{-T}_{t-1,t} \tag{17}$$

The new Kalman gain of Equation-18 and the new update covariance matrix equation of Equation-19 make use of the correlation expression from Equation-17 and the new measurement design matrix from Equation-14 as well as the new covariance matrix of Equation-16.

$$\mathbf{K}_t^{(+)} = (\mathbf{P}_t^{(-)} \mathbf{H}^T + \mathbf{C}_t)[\mathbf{H} \mathbf{P}_t^{(-)} \mathbf{H}^T + \mathbf{R} + \mathbf{H}_t \mathbf{C}_t + \mathbf{C}_t^T \mathbf{H}_t^T]^{-1} \tag{18}$$

$$\mathbf{P}_t^{(+)} = \mathbf{P}_t^{(-)} - \mathbf{K}_t[\mathbf{P}_t^{(-)}\mathbf{H}^T\mathbf{H} + \mathbf{R} + \mathbf{H}_t\mathbf{C}_t + \mathbf{C}_t^T\mathbf{H}_t^T]\mathbf{K}_t^T \tag{19}$$

$\mathbf{S}$, is the time correlation operator matrix. Hypothetically, if the measurement errors are not time-correlated, the $\mathbf{u}$ term will be absent. In other words, the measurement would contain white noise. The matrix $\mathbf{H}$ is the design matrix for time correlated measurements and $\mathbf{A}$ is the design matrix for measurement with no time-correlation. In our transport problem, where the state and measurement variable are the same entity, $\mathbf{A}$ matrix gives a linear relationship between the sate vector $\mathbf{x}$ and the measurement vector $\mathbf{z}$. Both $\mathbf{x}$ and $\mathbf{z}$ denotes the contaminant concentration vector. This leads to shape and construct the $\mathbf{A}$ matrix as a 0-1 matrix that has 1 in the cell having observation and 0 in the cell with no available observation. For each time step, if measurements are done with the same number of observation, which is most practical, the design matrix will remain the same at every time step. Again the design matrix for correlated measurement $\mathbf{H}$ will remain the same at every time step. Mathematically,

$$\mathbf{H}_{t-1} = \mathbf{H}_t = \mathbf{A}_{t-1} = \mathbf{A}_t .$$

Recalling the relationship between $\mathbf{S}$, $\mathbf{H}$ and $\mathbf{A}$ and using the above criterion.

$$\mathbf{H} = \mathbf{A}_t - \mathbf{S}_t\mathbf{A}_{t-1}\boldsymbol{\Phi}_{t-1,t}^{-1} = \mathbf{H} - \mathbf{S}_t\mathbf{H}\boldsymbol{\Phi}_{t-1,t}^{-1}$$

S must depend on **A** and **H** to keep the relation valid. In other words, the time correlation operator **S** is dependent on system operator **A** and the measurement operator **H**. There must exist an expression for **S** while it is treated as a matrix with unknown cell values, other than a matrix with some assigned value as stated earlier. An empirical expression for **S** is attempted to establish the following on the basis of this relational background along with the dimensional analysis of matrices. **A** is an $n' n$ square matrix. **H** is an $m' n$ rectangular matrix. Here n is the number of Eulerian nodes in the experimental space domain and m is the number of observation nodes. To make the matrices multiplication possible, the dimensions of the matrices need to be consistent. From the above expression, the following dimensional analysis of the matrices can be done.

$$Dim[\mathbf{H}] = Dim[\mathbf{H}] - Dim[\mathbf{S}]Dim[\mathbf{H}]Dim[\mathbf{\Phi}^{-1}_{t-1,t}]$$
$$m' \; n = m' \; n - [q' \; r][m' \; n][n' \; n] = m' \; n - [q' \; r][m' \; n]$$

To conduct a consistent matrix manipulation, q has to be equal to m and r has to be equal to m. Thus it is deducible that **S** is a $m' \; n$ square matrix.

Finally an expression for **S** is established as $m' \; n$.

$$\mathbf{S}_t = \boldsymbol{a}\, \mathbf{H}\mathbf{\Phi}_{t-1,t}\mathbf{H}^T$$

Here α is a scalar which stands for the correlation coefficient that lies between and along with 0 and 1. If there is no time-correlation in measurement errors, α is set to zero. In our transport problem, α =1/3 gives the least square error or the best fit prediction. This implies that the choosing of α is dependent on the extent of time correlation of the measurement error and needs model calibrations to have an accurate α .

Again,

$$Dim[\mathbf{S}_t] = Dim[\mathbf{H}]Dim[\mathbf{\Phi}_{t-1,t}]Dim[\mathbf{H}^T] = (m' \ n)(n' \ n)(n' \ m) = m' \ m$$

Which is identical to the earlier deduction of the dimension of $\mathbf{S}$.

3.6 Simulation Parameters

The contaminant transport simulation in the subsurface was carried out with parameter values adopted from Zou and Parr (1995). These parameters were used to generate results for both KF with Gaussian white noise and KF with time correlated measurement errors with the latter based on the measurement differencing approach by Petovello (2009). The model for this simulation is a 2 dimensional domain with a grid spacing of 1.524 m for both axes. The hydro-dynamic dispersions, $\mathbf{D}_x$ and $\mathbf{D}_y$ are 1.554 m^2day^{-1} and 0.4662 m^2day^{-1}, respectively. The flow velocity was assumed to be 1.054 $mday^{-1}$ in the $\mathbf{x}$ direction. The porosity ($\boldsymbol{\mu}$), aquifer thickness ($\mathbf{b}$) and time interval for each time step were set at 0.3, 6.1 m and 0.2 day, respectively. The correlation coefficient

matrix ($\mathbf{S}$) and retardation ($\mathbf{R}$) were set at 1/3 and 1 for running a total of 50 time step simulation. The value of the correlation parameter was chosen based on trial and error. For a more practical and realistic consideration, 9 sparse measurement data set was used to predict the simulation area of 400 nodes. Finally, a standard deviation of 4 mg/L and 2.5 mg/L was applied as the process errors and observation errors, respectively. The initial concentration of the conservative pollutant occurring as a spill was 10,000 mg/L and is assumed to occur at grid point (5, 10) in the 20×20 space domain. Simulations were carried out by writing codes for numerical, reference true field (which is based on analytical solution with added random errors), Kalman filter with Gaussian noise and Kalman filter with time correlated measurement errors.

3.7 Performance Indicator

The root mean square error (RMSE) was used as an indicator to measure the performance of the KF with Gaussian white noise, KF with colored noise measurement errors and numerical results relative to the true solution in the entire space and time domain. The RMSE results of these three simulations were then compared and contrasted with each other in prediction results and unique behavior of RMSE for particular time-steps of interest.

$$\mathbf{RMSE} = \sqrt{\frac{\mathbf{1}}{\mathbf{N_t - 1}} \sum \left[\mathbf{C^E(x,y,t) - C(x,y,t)} \right]^2} \tag{20}$$

In this case, the total number of sampling nodes is, $\mathbf{N_t}$, where $\mathbf{C(x,y,t)}$ and $\mathbf{C^E(x,y,t)}$ are the reference true values and estimated values, respectively in the two dimensional plane $\mathbf{(x,y)}$ for a particular time $\mathbf{t}$.

CHAPTER 4

RESULTS AND DISCUSSION

It is assumed that all the parameters in both the KF with white Gaussian noise and the KF with time correlated measurement errors are all known or derived for this study. This implies that the measurement design matrix $\mathbf{H}$, the covariance $\mathbf{Q}$ and $\mathbf{R}$ for the process noise and measurement noise, respectively and all other parameters in both filter algorithms are all known including the $\boldsymbol{a}$ for the $\mathbf{S}$ matrix. The initial concentration at the time of spill is known. Several simulations were conducted to verify the possibility and efficiency in predicting contaminant transport in the subsurface by comparing the measurement differencing algorithm by Petovello (2009) to the standard Kalman filter.

4.1 Simulation Output

There was a significant improvement in plume prediction for both filters compared to the FTCS results for all time steps, as shown in Figures 4.1 through 4.9, which represent the concentration profile from the numerical KF and KF with colored noise for time steps 10, 20 and 30 respectively. Taking a closer look at the contour profiles for the two filters suggest an optimum performance of the KF with correlated or colored measurement noise as the time steps increases. On the other hand, the apparent poor performance of the FTCS model can mainly be attributed to numerical errors. As explained by Spitz and Moreno (1996), there are several sources of errors in numerical models. To mention a few, we have truncation errors, round off errors, distance-related

dispersion errors and instability. Truncation errors occur when a complex function such as concentration is expressed as a series of simpler functions. Round off errors may also be a very significant reason for the out-put of the numerical results. Rounding off has the tendency of accumulating with time, hence causing numerical instability. Errors due to distance-related dispersion originate in all finite difference (FD) models including FTCS because grid concentrations are only known at the nodes that represents an entire cell. Finally there is the issue of instability which results in a feed-back process which accumulates the errors for every step taken to obtain the final results. Any of these sources of numerical errors discussed above could have been the reason for the numerical results output. There are several other possible sources of numerical errors that have not been addressed in this research. More information on other types of numerical errors can be found in Spitz and Moreno (1996).

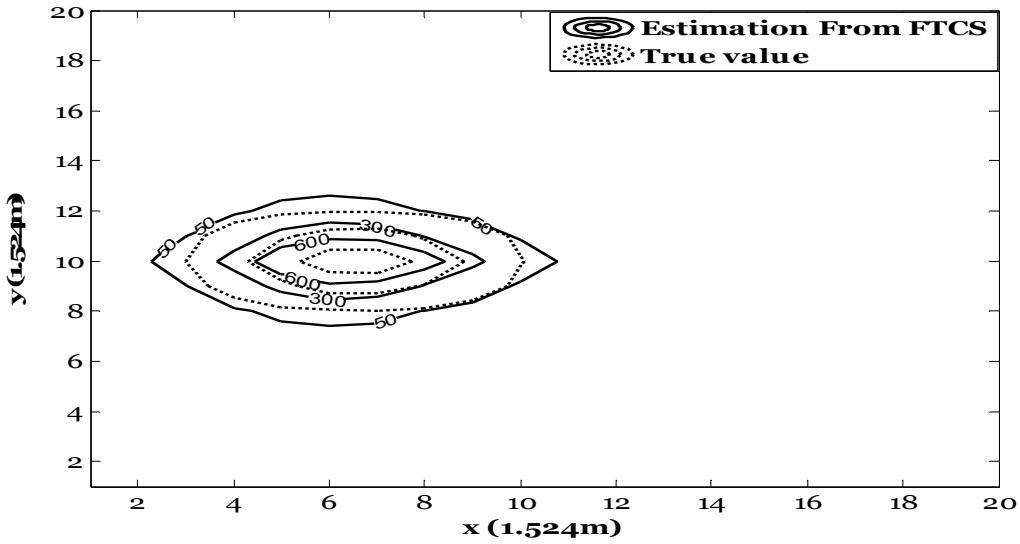

Figure 4.1 Plume prediction by FTCS and analytical (true value) methods at time step 10

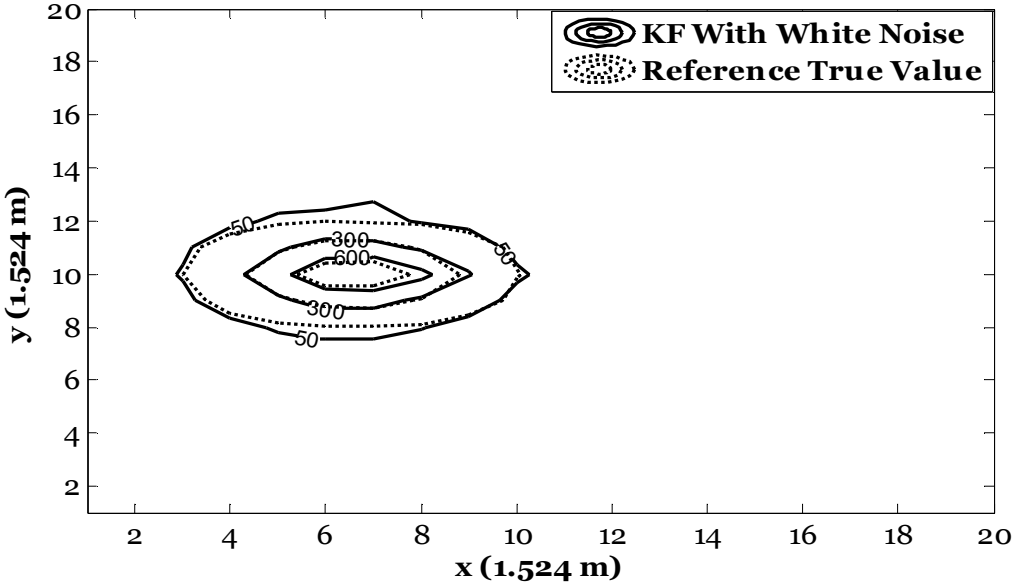

Figure 4.2 Plume prediction by KF and analytical (true value) methods at time step 10

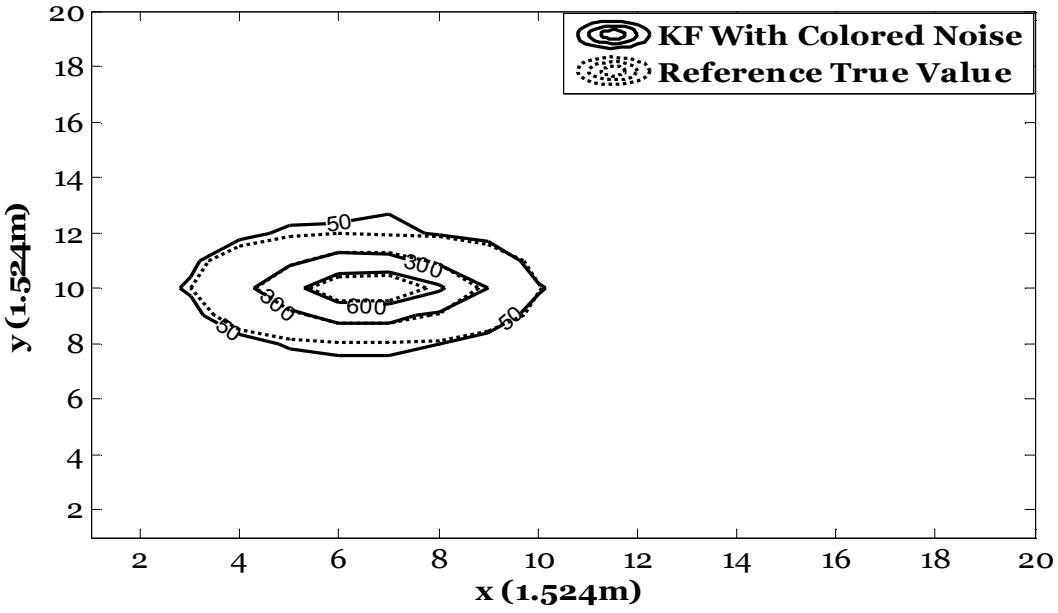

Figure 4.3 Plume prediction by KF with colored measurement noise and analytical (true value) methods at time step 10

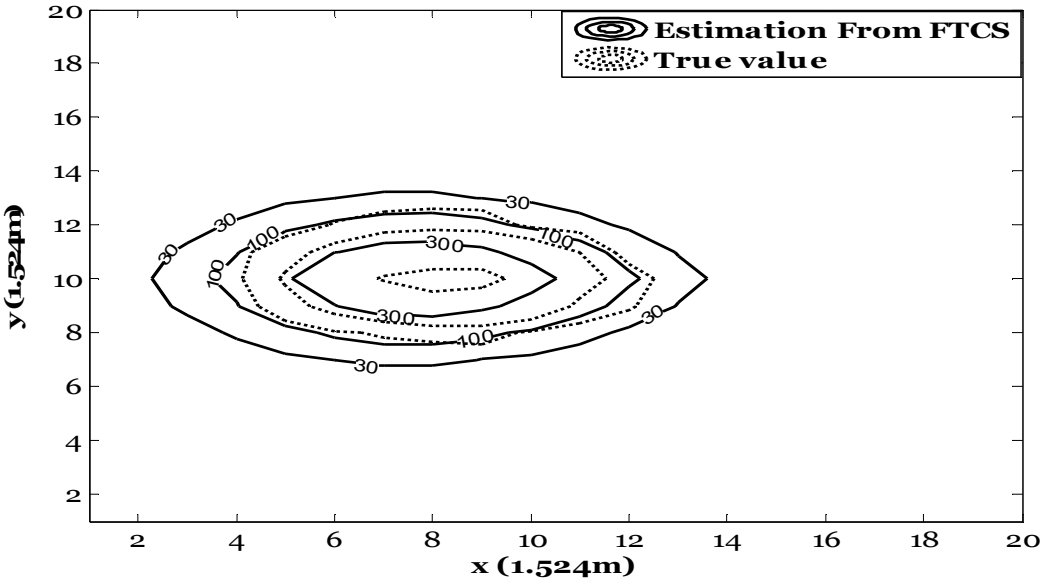

Figure 4.4 Plume prediction by FTCS and analytical (true value) methods at time step 20

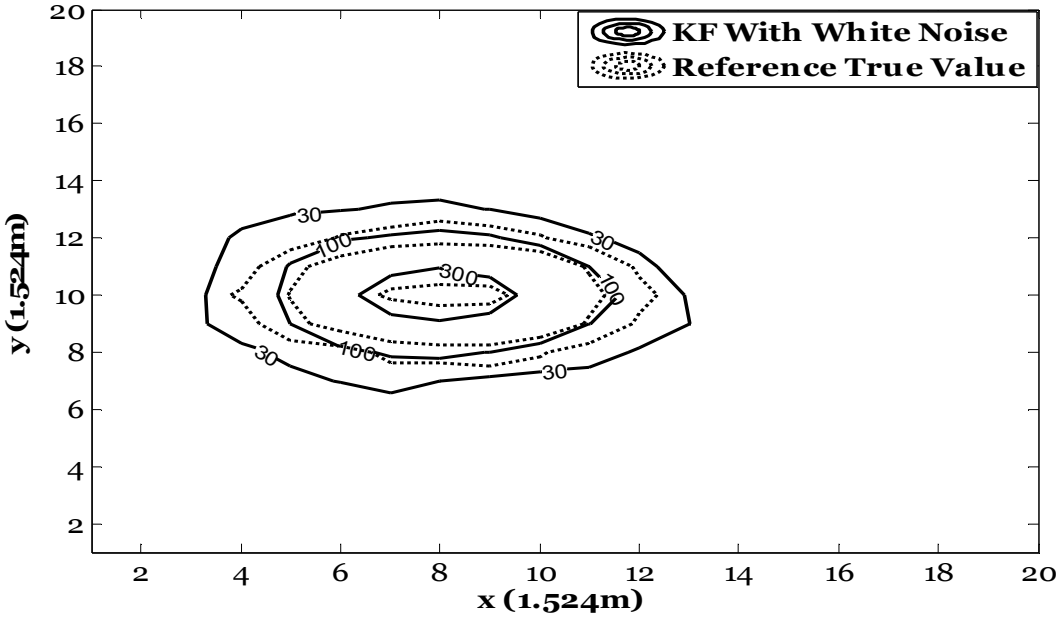

Figure 4.5 Plume prediction by KF and analytical (true value) methods at time step 20

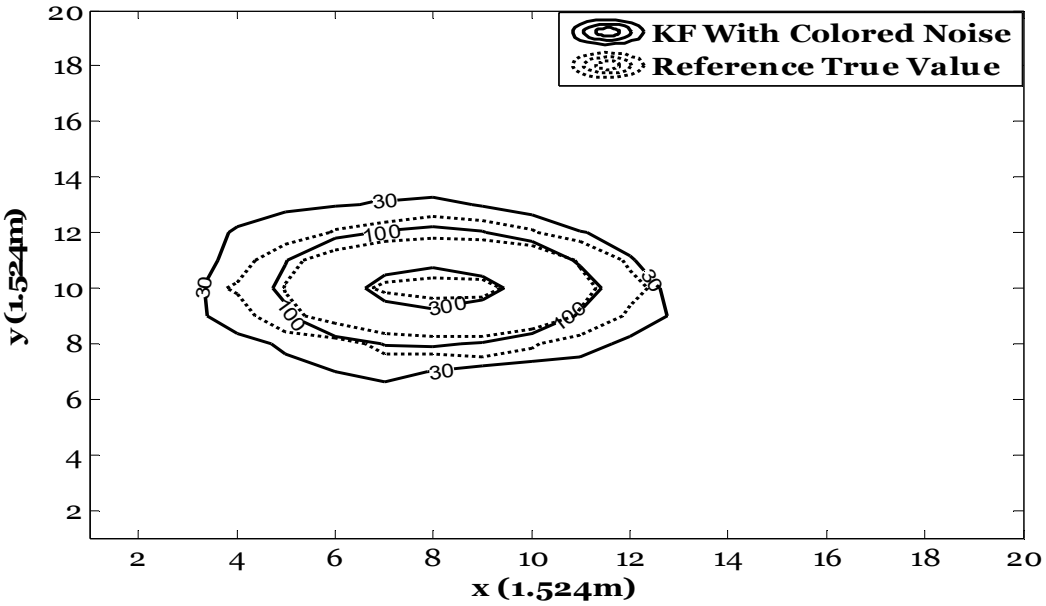

Figure 4.6 Plume prediction by KF with colored measurement noise and analytical (true value) methods at time step 20

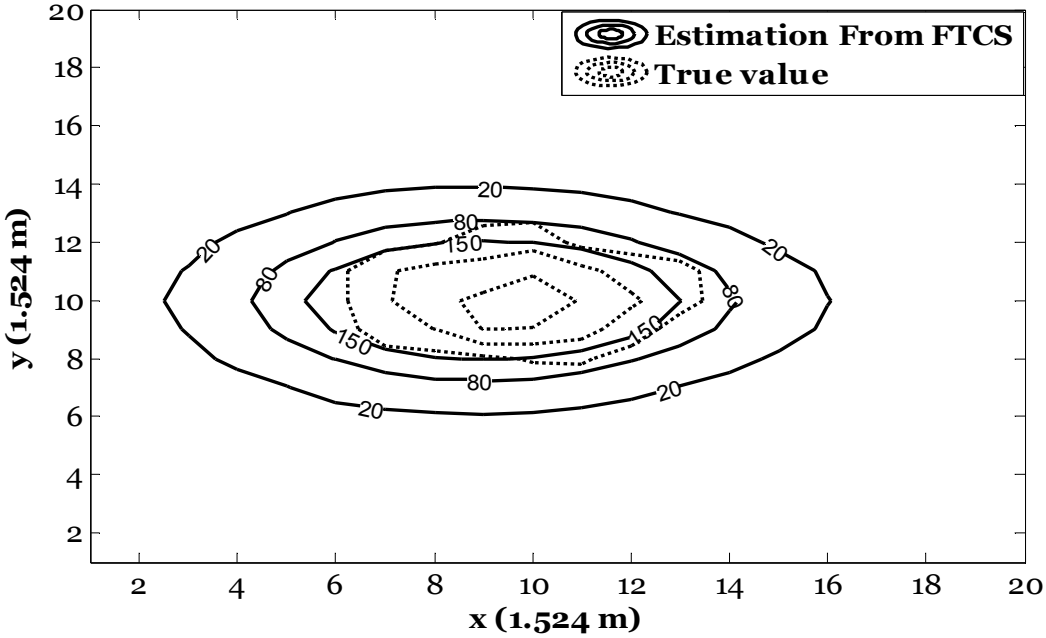

Figure 4.7 Plume prediction by FTCS and analytical (true value) methods at time step 30

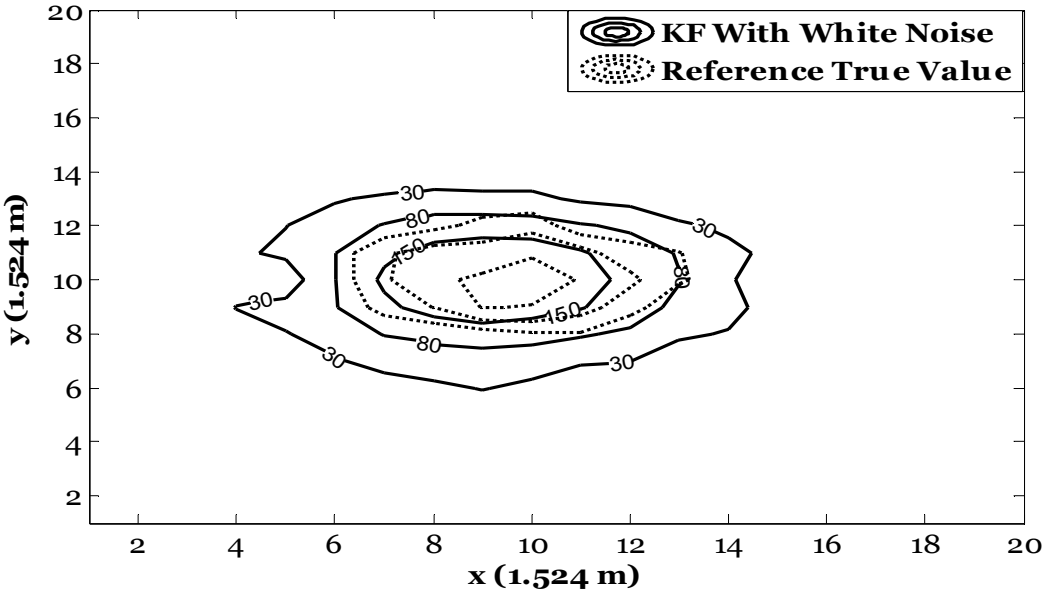

Figure 4.8 Plume prediction by KF and analytical (true value) methods at time step 30

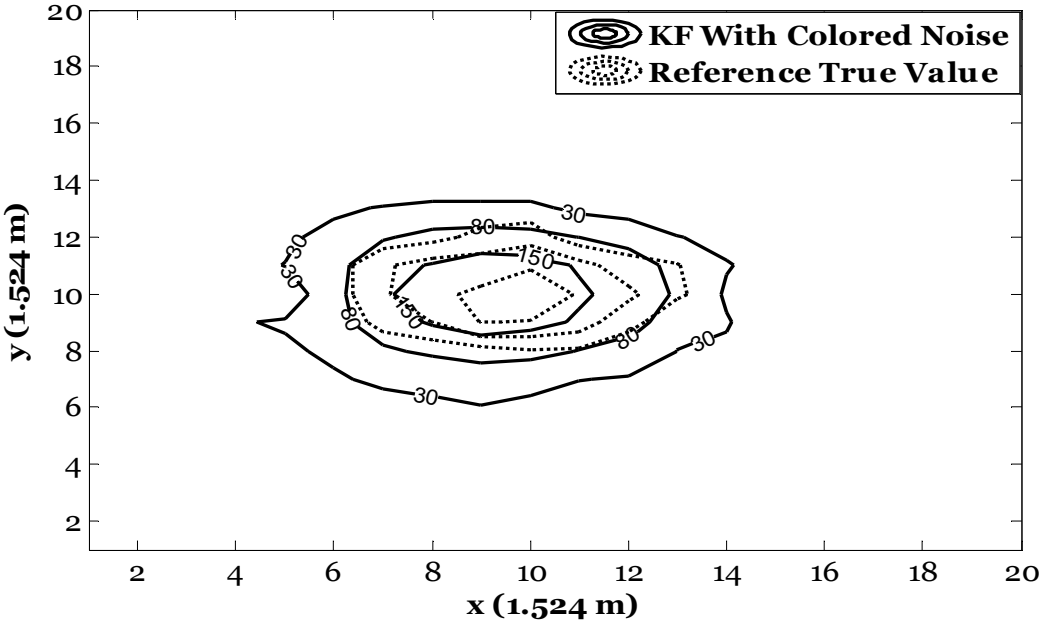

Figure 4.9 Plume prediction by KF with colored measurement noise and analytical (true value) methods at time step 30

4.2 Root Mean Square Error Analysis

Simulation results obtained from KF with white Gaussian errors and KF with time correlated Gaussian errors look very close in terms of contour description but the RMSE profile in Figure 4.10 indicates that the later has slightly improved performance over the former. Relative to the numerical solution, the KF with white noise improved the prediction by an average of 51.5% while the Kalman filter with correlated errors improved the prediction by an average of 62.9% in the total simulation time steps of 50 using 9 observation points in the entire 20×20 space domain. Relative to the numerical results, the KF with correlated errors therefore reduces the errors in prediction by 11.4% compared to the KF with white Gaussian noise. Between time-steps zero and four, the Kalman filter with colored noise reduced the errors of the Kalman filter by 15% with time step 4 having the highest error reduction of 24% in this range. After time step 4 the error difference reduced steadily to time step 6 and remained nearly constant at about 17% till time step 26. From these results, the measurement differencing approach to deriving a filter that takes into account correlated measurement noise proves to be superior in predicting contaminant transport in the subsurface in cases of correlated measurement errors than the ordinary Kalman filter which assumes white Gaussian noise with characteristics of no correlation. Note that in the event of colored measurement observations in contaminant transport data, it will be more appropriate to consider using the KF with the measurement differencing approach since this fully takes into account the time correlated nature of the observations. Since the use of GPS equipment is very common these days in taking field data that contain different time correlated errors

including clock errors and orbital errors (Olynik et al 2002), it can be assumed that most of these data are correlated to some extent even though further investigation needs to be carried out to ascertain the level of correlation or the extent of the colored noise available in the measured field data.

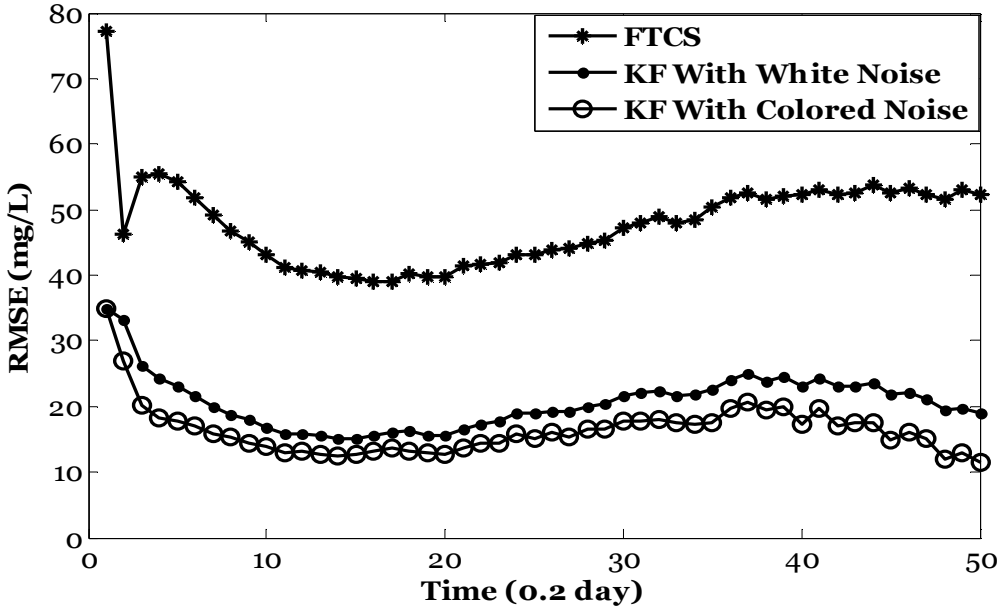

Figure 4.10 RMSE profile for FTCS, KF and KF with colored measurement noise

The performance of the filters and numerical solution with was further investigated under three scenarios by performing sensitivity analysis on it. The different sensitivities conducted are listed below;

1. by altering the observation noise standard deviation for the KF with time correlated errors

2. by changing the process noise standard deviation of the KF with time correlated errors

3. Stability and Convergence Analysis

4.3 Altering Observation Noise

By varying the observation noise standard deviation for KF with correlated errors by specified amounts while maintaining the same process noise standard deviation, the results of the performance was analyzed as indicated in Figure 4.11. The standard deviation of observation noise (SDON) was set at 1, 6, 12 and 18 mg/l, respectively for a constant process noise standard deviation of 4 mg/l. For increasing observation noise standard deviation, it was observed that the RMSE results for the respective correlated error filters were much close at the end of the of the 50 time steps. The highest difference in results occurred at time step 1, with the standard deviation of 1 mg/l producing very optimistic results. Using a standard deviation of 1 mg/L improved the performance of the filter by about 29.5% relative to the RMSE results obtained with a standard deviation of 6mg/l of the observation noise. Relative to the RMSE results produced with a standard deviation of 12 mg/L and 18 mg/L, the results obtained with the standard deviation of 1 mg/L were improved by approximately 60.6% and 64.5%, respectively. This made sense for an increased standard deviation in observation; one should expect slightly decreased prediction efficiency of the filter.

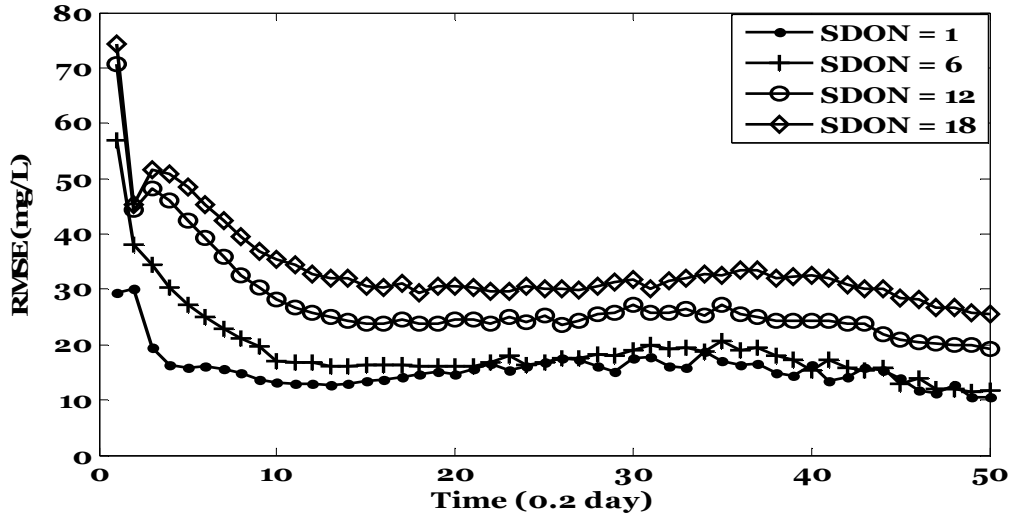

Figure 4.11 RMSE profile of KF with time correlated measurement noise for different standard deviation of observation noise (SDON) values

4.4 Altering Process Noise

The influences of the process noise standard deviation (PNSD) on the result of the KF with correlated measurement errors was investigated by simulating the KF with correlated errors with different process error standard deviations as in the previous investigation. The standard deviation in the process noise was made (1 mg/L, 6 mg/L, 12 mg/L) and finally 18 mg/L for different simulations, while the standard deviation of the observation noise was made constant for every simulation at a value of 2.5 mg/L. The result of the analysis is shown on Figure 4.12. For the first two scenarios, there was a significant change in performance of the result of the filter. The process noise standard deviation of 6 mg/L had a better output than the 1 mg/L standard deviation from time step 1 to time step 13 (about 35% difference). Even though from time step 13 to time step 50

the RMSE profile of the 1 mg/L standard deviation appears to be slightly better than the 6 mg/L standard deviation, the difference is approximately 2%. So on the average, the second scenario had a better improved RMSE profile than the first scenario. The third scenario initially had an optimistic RMSE profile from time step 1 to time step 7 relative to the first scenario (about 26% difference), but beyond this range, the first scenario performance surpassed the third by approximately 57.7% for the remaining time steps, which makes the first scenario still superior in performance over the third. The result of the fourth scenario was much worse than the previous two relative to the first scenario. From time step 1 to time step 6 it proved to be better than the first scenario by about 18% but for the remaining time steps it performed about 71% worse than the first scenario. All 4 scenarios arranged in order of performance superiority will be (6 mg/L and 1 mg/L) which are very close, followed by 12 mg/L and finally 18 mg/L the least of them all.

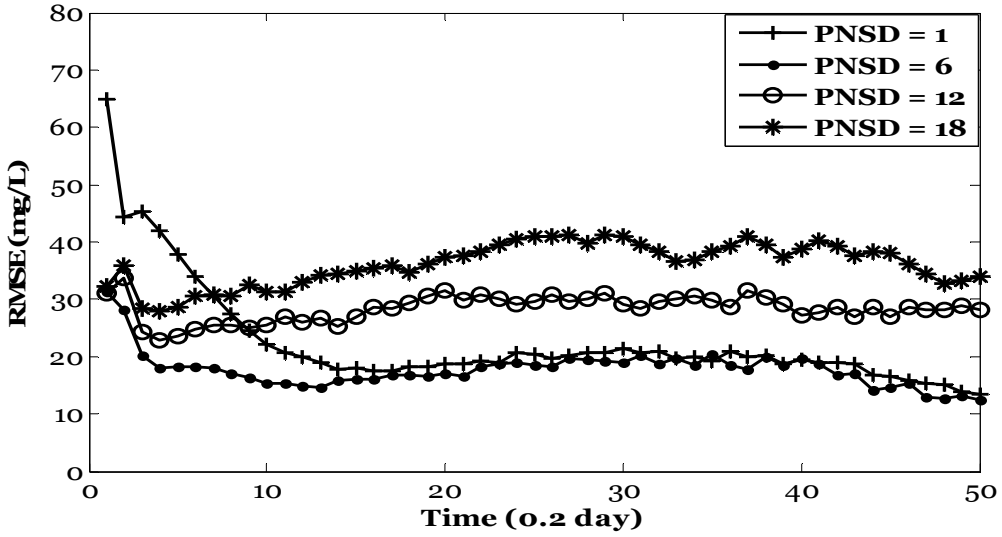

Figure 4.12 RMSE profile of KF with colored measurement noise for different process noise standard deviation (PNSD) values

4.5 Stability and Convergence Analysis

Figures 4.13, 4.14 and 4.15 show the convergence and stability of the numerical, KF with white Gaussian noise and KF with time correlated errors for a series of multiple runs. All the three results were fairly stable and also convergent as it can be seen in the RMSE profiles. This makes the comparison between the three results in terms of their stability and convergence unbiased.

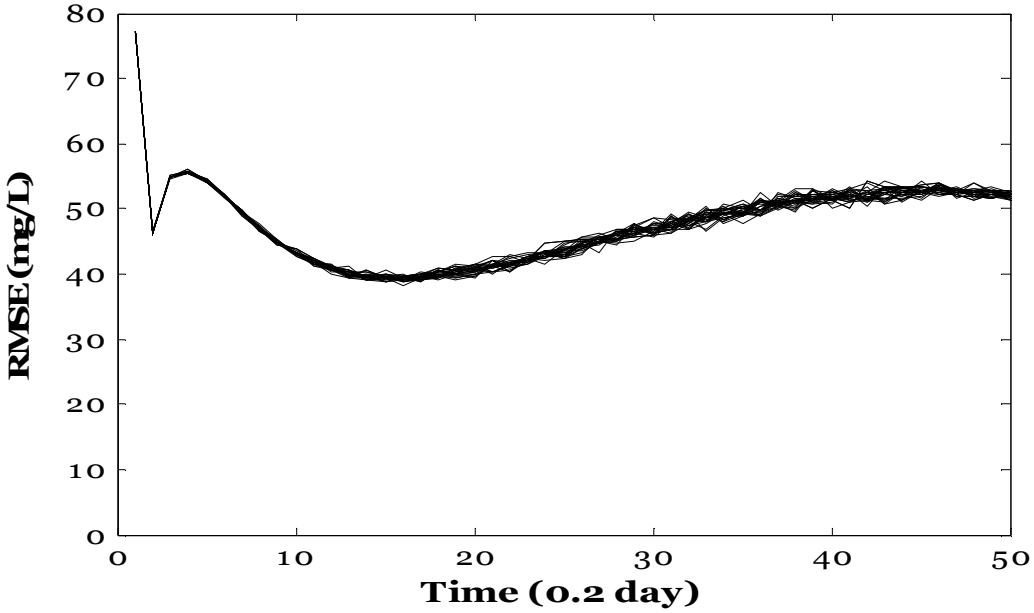

Figure 4.13 10 Runs of RMSE of FTCS

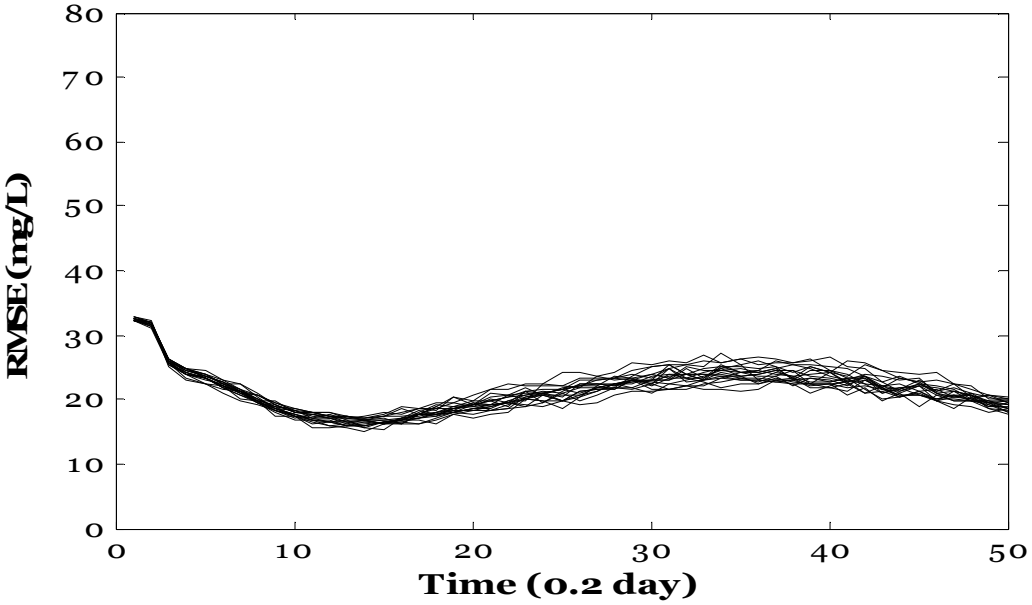

Figure 4.14 10 Runs of RMSE of KF with white noise

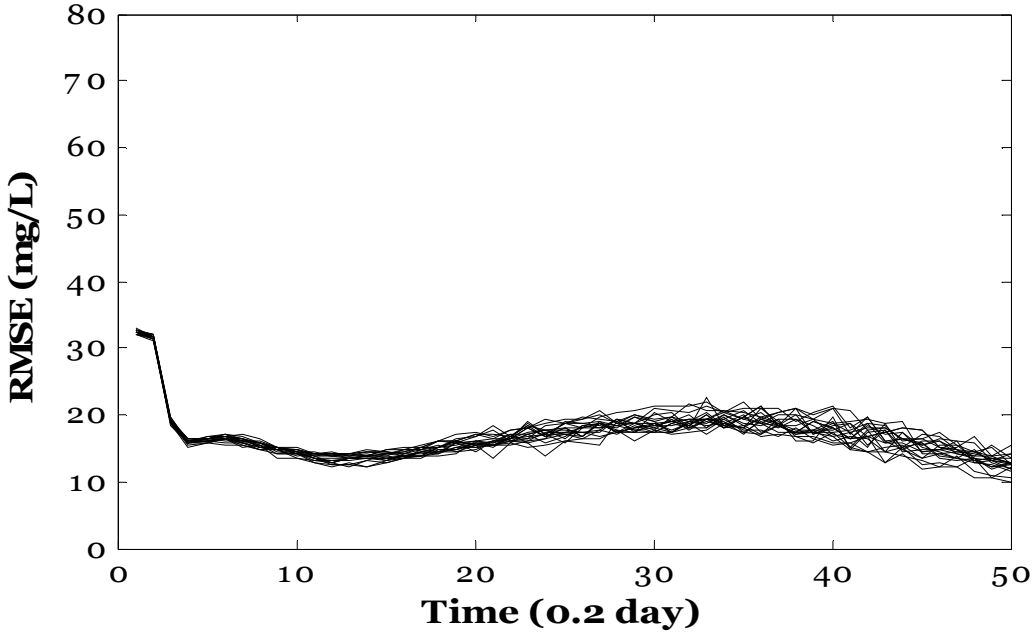

Figure 4.15 10 Runs of RMSE of KF with colored measurement noise

CHAPTER 5

CONCLUSION

There have been several instances that hydrological data has been found to be corrupted with time correlated measurement errors. For measurement errors that are correlated, in other words if the measurement data is corrupted by errors that are time dependent, the measurement differencing technique can effectively be applied to give a better prediction than the normal Kalman filter. The Kalman filter can only assume white Gaussian measurement and process errors; hence it does not take into account time correlated errors.

In this research one of the effective methodologies for applying data assimilation to an observed data that is characterized by time correlated measurement errors is investigated. The numerical advection dispersion equation was modified by adding a noise term and used as the process equation. The observation equation was derived from the 2 dimensional dispersion advection contaminant transport equation which was corrupted with random errors that have a time function. The investigation is carried out in the prediction of fate and transport of contaminant in time and in space within the subsurface by the measurement differencing method. Simulations of both filters were carried out using a two-dimensional model describing the subsurface contaminant transport of a conservative solute.

First, the result of the two filters showed that the KF with time correlated measurement errors was slightly superior over the KF with white noise by about 11.4%.

Further investigation revealed that the performance of the KF with correlated measurement is enhanced when the observation errors standard deviation is made minimum by using 1 mg/L compared to when it is set at 8 mg/L, 12 mg/L and 18 mg/L. Much the same way, the results in performance of the KF with correlated errors improved when the process error standard deviation was made minimum (at 1 mg/L) in contrast to higher process noise values.

An important consideration in running the measurement differencing algorithm is the correlation coefficient value and the inverse of the state transition matrix. For purposes of stability, a $\mathbf{S}$ matrix needs to be formulated with a calibrated correlation coefficient value appropriate for a particular measurement data. The only considerable hurdle to overcome is to ensure that the inverse of the state transition matrix '$\mathbf{\Phi}$' can be computed since this is needed in the measurement differencing algorithm. Nevertheless, the measurement difference algorithm is very helpful when considering time correlated measurement.

For establishing the stability and convergence criteria of the results, a series of multiple RMSE runs of the results was conducted. At time step 50, all three results (FTCS, KF with white Gaussian errors and KF with time correlated errors) converged and were stable with minimal instability. In the near future, new algorithms for adaptive, extended and ensemble KF that consider time correlated measurement errors can be applied in subsurface contaminant transport to investigate their performance and potential to improve subsurface contaminant transport. Finally, these algorithms can also be explored on a bigger scale to yield more realistic results.

REFERENCES

Billah, K. Y., and Shinozuka, M. (1990). "Numerical methods for colored-noise generation and its application to a bistable system." *Phys. Rev.,* A42(12), 7492-7495.

Bryson, A. E. Jr., and Henrikson, L. J. (1968). "Estimation using sampled data containing sequentially correlated noise." *J. Spacecraft and Rockets.,*5(6), 662-665.

Brown, R. G., and Hwang, P. Y. C. (1997). *Introduction to random signals and applied Kalman filtering with MATLAB exercises and solutions,* 3rd Ed., John Wiley &Sons Inc., USA.

Chang, S. Y., and Jin., A. (2005). "Kalman filtering with regional noise to improve accuracy of contaminant transport models." *J. Environ. Eng.,*131(6), 971-982.

Chang, S. Y., and Latif, S. M. I. (2007). "Use of Kalman filtering and particle filtering in a one dimensional leachate transport model." *Proc.,3rd National Conf. on Environmental Science and Technology.*, Springer, Greensboro, NC.

Chang, S. Y., and Latif, S. M. I. (2010). "Extended Kalman filtering to improve the accuracy of a subsurface contaminant transport model." *J. Environ Eng.,* 136(5), 466-474.

Charles, W. M,. Heemink, A. W., and van den Berg, E. (2008)."Colored noise for dispersion of contaminants in shallow waters." *J. Applied Mathematical Modeling.,* 33 (2) 1158-1171.

Drecourt, J. F. (2003). "Kalman filtering in hydrological modeling." *DAIHM, Tech. Rep. No.1.,* DHI water and environment.,Denmark.

Drecourt, J. F., Madison, H., and Rosbjerg, D. (2006). "Calibration framework for a Kalman filter applied to a groundwater model." *Adv. Water Resour.,* 719–734.

Eppstein, M. J., and Dougherty, D. E. (1996). "Simultaneous Estimation of Transmissivity Values and Zonation." *Water Resour. Res.*, 32(11), 3321-3336.

Ferraresi, M., Todini, E., and Vignoli, R. (1996). "A solution to the inverse problem in groundwater hydrology based on Kalman filtering." *J. Hydrol*., 175(1-4), 567-581.

Ganguly, C., Matsumoto, M. R., Rabideau, A. J., and Van Benschoten, J. E. (1998). "Metal ion leaching from contaminated soils: 1. Model development," *J. Environ .Eng.*, 124(3),278-287.

Ganguly, C., Matsumoto, M. R., Rabideau, A. J., and Van Benschoten, J. E. (1998). "Metal ion leaching from contaminated soils: 2. Model application to lead contaminated soils," *J. Environ. Eng.*, 124(12), 1150-1158.

Gelb, A. (1974). *Applied optimal estimation*, The MIT Press, Cambridge.

Geogebeur, M., and Pauwels, V. R. N. (2007). "Improvement of the PEST parameter estimation algorithm through Extended Kalman filtering." *J. Hydrol.,* 337, 436-451.

Geer, F. C. V. (1982). "An Equation based theoretical approach to network design for groundwater levels using kalman filters." *International Association of Hydrological Sciences*, 136, 241-250.

Graham, W., and McLaughlin, D. (1989). "Stochastic analysis of nonstationary subsurface solute transport: 2. Conditional moments." *Water Resour. Res.*, 25(11), 2331-2355.

Hossain, M. A., and Yonge, D. R. (1997). "Linear Finite-Element Modeling of Contaminant Transport in Ground Water." *J. Environ. Eng.*, 123 (11), 1126-1135.

Huang, M. C., Wu, J. W., Luo, Y. P., and Petrosyan, K. G. (2010). "Fluctuations in gene regulatory networks as gaussian colored noise." *J. Chem Phys.,* 132(15), 155101.

Johnson, D. J. (1970). "Application of a Colored Noise Kalman filter to a Radio-Guided Ascent Mission." *J. Spacecraft and Rockets*., 7, 277.

Johnson, J,. and Dinardo, J. (1996). *Econometric Methods,* N. Y. McGraw-Hill.

Kalman, R. E. (1960). "A New Approach to Linear Filtering and Prediction Problems." *J. Basic Eng.*, 82(1) 35-45.

Kuhlmann, H. (2003). "Kalman-Filtering with colored measurement noise for deformation Analysis." *11th FIGInternational Symposium on Deformation Measurements*, Santorini,Greece.

Kumar, A., and Crassidis, J. L. (2007). "Colored-Noise Kalman filter for Vibration Mitigation of Position/Attitude Estimation Systems." *AIAA Guidance, Navigation and Control Conference and Exhibit*, Hilton Head, S. C.

Kochendorfer, J. P., and Ramirez, J. A. (2003). "Modeling the continental-scale dynamics of the coupled land-surface and atmospheric water balances with a stochastic differential Equation." Water Resources, Hydrologic and Environmental Sciences Division, Civil Engineering Department, Colorado State University, Ft Collins.

Lee, K. Y. (2004). “Modeling long-term transport of contaminants resulting from dissolution of a coal tar pool in saturated porous media.” *J. Environ. Eng.*, 130(12), 1507-1513.

Ngan, P., and Russel, S. O. (1986). “Examples of floating forecast with Kalman filter.” *J. Hydrol Eng.,* 112(9), 818-832.

Olynik, M., Petovello, M. G., Cannon, M. E., and Lachapelle, G. (2002). “The effect of GPS errors on relative single point positioning over time.” *GPS Solut.,* 6(1-2), 47-57.

Paola, M. R., and Eli, T. (1996). “The oceanographic data assimilation problem: Overview, motivation, and purposes.” *Modern Approaches to Data Assimilation in Ocean Modeling,* 3–17. Elsevier Science B.V., Amsterdam.

Petovello, M. G., O’Keefe, K., Lachapelle, G., and Cannon, M. E. (2009). “Consideration of time-correlated errors in Kalman filter applicable to GNSS.” *J. Geod.,* 83, 51-56.

Pimentel, K. D., Candy, J. V., Azevedo, S. G., and Doerr, T. A. (1982). "Simplified groundwater flow modeling: An application of Kalman filter based identification." *Mathematics and Computers in Simulation*, 24(2-3), 140-151.

Popescu, D. C., and Zeljkovic, L. (1998). “Kalman filtering of colored noise for speech Enhancement.” *Proc., IEEE International Conference on Acoustics, Speech and Signal Processing,* Seattle, WA., 997-1000.

Rabideau, A. J., and Khandelwal, A. (1998). “Boundary conditions for modeling contaminant transport in vertical barriers,” *J. Environ. Eng.*, 124(11), 1135-1141.

Robinson, A. R., and Lermusiaux, P. F. J. (2000). *Overview of data assimilation*. Harvard Reports in Physical/Interdisciplinary Ocean Science, 62.

Schwartz, F. W., and Zhang, H. (1994). *Fundamentals of groundwater,* Wiley, New York.

Simon, D. (2006). *Optimal state estimation. kalman, H Infinity, and nonlinear approaches*, John Wiley & Sons, Inc., Hoboken, New Jersey.

Solo-Gabriele, H. M. A. (1998). “Generation of long-term record of contaminant transport.” *J. Environ. Eng*., 124(7), 619-627.

Spitz, K., and Moreno, J. (1996). *A practical guide to groundwater and solute transport modeling,* John Wiley & Sons, Inc. New York.

Sun, S. L., and Deng, Z. L. (2004). "Optimal fusion Kalman filter for systems with colored measurement noises." *Proc., 5th World Congress on Intelligent Control& Automation, Hangzhou, China*, 1562-1566.

United States Geological Survey. (2009). "Summary of estimated water use in the United States in 2005".

Van Geer, F. C., and Van Der Kloet, P. (1985). "Two algorithms for parameter estimation in groundwater flow problems." *J. Hydrol.*, 77(1-4), 361-378.

Van Geer, F. C., Te Stroet, C. B. M., and Yangxiao, Z. (1991). "Using Kalman Filtering to Improve and Quantify the Uncertainty of Numerical Groundwater Simulations: 1. The Role of System Noise and Its Calibration." *Water Resour. Res.*, 27(8), 1987-1994.

VanKampen, N. G. (1992). *Stochastic processes in physics and chemistry*. North-Holland Publishing, Amsterdam.

Wang, J., Bras, R. L., and Entekhabi, D. (1997). "Structure in fluctuations of large scale soil moisture climate due to external random forcing and internal feedbacks." *Stoch. Hydrol. Hydrau.,* 11, 95-114.

Wang, K., Li, Y., and Rizos, C. (2010). "The practical approaches to kalman filtering with time-correlated measurement errors." *Unpublished.,* Beihang University, Beijing 100191, China, University of new South Wales Sidney NSW 2052, Australia.http://www.gmat.unsw.edu.au/snap/publications/wangk_etal2010a.pdf. (Nov.17, 2010).

Wang, R. Y., and Cho, C. M. (1999). "The Kalman filter with colored noise and its application to flood forcasting of a river basin." *Proc., Joint Congress, 2nd International Conference on Water Resources and Environmental Research and 25th Hydrology and Water Resources Symposium.Water 99, Australia.*

Welch, G., and Bishop, G. (2006). "An Introduction to the Kalman filter." *Tech. Rep. No.TR95- 041*.University of North Carolina, Department of Computer Science, http://www.cs.unc.edu/~welch/media/pdf/Kalman_intro.pdf. (Feb. 12, 2010).

Yan, J. M., Vairavamoorthy, K. and Gorantiwar, S. D. (2006). "Contaminant transport model for unsaturated soil using fuzzy approach." *J. Environ. Eng*., 132 (11), 1489-1497.

Yu, Y. S., Guang-Te, W. and Heidari, M. (1989). "Optimal estimation of contaminant transport in groundwater." *Water Resour. Bull.* 25, 295-300.

Zou, S., and Parr, A. (1995). "Optimal estimation of two-dimensional contaminant transport." *Groundwater*, 33(2), 319-325.